A Theoretical Investigation of the Methylation of Methylbenzenes and Alkenes by Halomethanes over Acidic Zeolites

Stian Svelle,[†] Stein Kolboe,*[,†] Unni Olsbye,[†] and Ole Swang[‡]

Department of Chemistry, University of Oslo, P.O. Box 1033 Blindern, N-0315 Oslo, Norway, and SINTEF Applied Chemistry, Department of Hydrocarbon Process Chemistry, P.O. Box 124 Blindern, N-0134 Oslo, Norway

Received: January 24, 2003; In Final Form: March 17, 2003

The reactivity of chloromethane, bromomethane, and iodomethane over acidic zeolite catalysts has been probed, using the methylation of ethene, propene, and toluene as model reactions. Adsorbed reactants, transition states, and adsorbed products have been investigated. A cluster model has been used to represent the zeolite. Both the associative (direct) mechanism and the dissociative mechanism (via the formation of surface methoxide groups) have been studied. Quantum chemistry predicts that the associative pathway is favored over the dissociative mechanism. A weak trend in reactivity is found among the halomethanes, indicating the following order of reactivity: MeI > MeBr > MeCl. The results are compared with recent theoretical studies on methanol reactivity.

1. Introduction

The proven world reserves of natural gas (mainly methane) are of equal magnitude to those of oil.[1] Therefore, activation of methane and subsequent conversion of activated methane to higher hydrocarbons or other value-added products is a research area to which considerable effort has been devoted.[2] Currently, most such routes of gas upgrading proceed via the formation of synthesis gas ($CO + H_2$). This step may be achieved by steam reforming of methane using a supported nickel catalyst.[3] The reaction temperature employed is 800−900 °C, which might result in a considerable loss of energy during heat transfer processes. Synthesis gas may be reacted into higher hydrocarbons using Fischer−Tropsch technology, employing various metal catalysts.[4] An alternative route involves $Cu/Zn/Al_2O_3$ catalyzed synthesis of methanol from synthesis gas[5] and subsequent conversion of methanol to hydrocarbons (MTH).[6,7] Depending on product demand, methanol can be reacted into a gasoline range mixture of hydrocarbons (methanol to gasoline, MTG) using the acidic H-ZSM-5 catalyst or to a product mixture consisting mainly of ethene and propene (methanol to olefins, MTO) by employing acidic H-SAPO-34 catalysts.[6,7]

Circumvention of the costly formation of synthesis gas might be achieved, however, by transforming methane directly into monosubstituted halomethanes. This is possible through the oxyhydrochlorination (OHC) process,[8] where methane is reacted with hydrogen chloride and oxygen to form chloromethane and water over a supported copper chloride catalyst. Chloromethane may also be produced by monohalogenation of methane over supported platinum metal catalysts.[9] In the second step, chloromethane, or any halomethane, may be converted to hydrocarbons and hydrogen halides over acidic microporous catalysts, for instance H-SAPO-34 or H-ZSM-5. The produced hydrogen halide may then be separated from the hydrocarbon product and recycled back to the halogenation process step.[8] Formation of water as byproduct, which constitutes 55.6% (by weight) of the products in methanol conversion, is thereby avoided.

Early patents, mainly describing the conversion of methanol to hydrocarbons over acidic zeolites, also mention the possibility of converting halomethanes.[10,11] Some reports also exist in the regular scientific literature, mainly focusing on chloromethane as reactant.[12−22] Utilizing bromomethane or iodomethane as possible reactants is occasionally mentioned,[23] but little experimental data are available for comparison between the three. Murray et al.[24] have found that the order of reactivity follows the expected leaving group trend (MeI > MeBr > MeCl). However, the catalysts used were alkali-exchanged zeolites, and a comparison with purely proton-exchanged zeolites may not be valid.

There does not appear to be a clear consensus on whether halogen atoms are incorporated in the hydrocarbons produced or not. It has been reported that up to 4% of the product from chloromethane conversion contained halogen,[13,14,18,22] while Lersch and Bandermann[16] did not detect any chlorinated products. Minimizing the amount of halogenated products is beneficial from an industrial and environmental viewpoint.

Many articles on the subject point out the similarities in product distribution, and probably also in reaction mechanism, between methanol and halomethane conversion.[12,13,15,16,18,21] These similarities will also be drawn upon in the present work. Recently, great progress has been made regarding the mechanistic description of methanol conversion. Dahl and Kolboe[25] have formulated a "hydrocarbon pool" mechanism, where methanol is continuously added to an adsorbate inside the zeolite pores, followed by production of alkenes via subsequent dealkylations of the adsorbate. The specific nature of the hydrocarbon pool has been clarified in a series of publications from Kolboe and co-workers,[26] Haw and co-workers,[27] and Hunger and co-workers.[28] It appears that polymethylbenzenes, polymethylnaphthalenes, polymethylated cyclopentenyl ions, and, in some cases, aliphatic species can constitute the hydrocarbon pool. There may also be a facile interconversion of these

* Corresponding author. E-mail: stein.kolboe@kjemi.uio.no.
[†] University of Oslo.
[‡] SINTEF Applied Chemistry.

10.1021/jp030101u CCC: $25.00
Published on Web 05/09/2003

SCHEME 1: Catalytic Cycle of the "Hydrocarbon Pool" Mechanism[a]

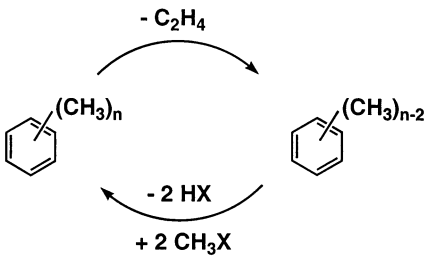

[a] In the present work, we have investigated the methylation of compounds known to exist inside the zeolite pores during halomethane conversion.

hydrocarbon pool species. The hydrocarbon pool mechanism is clarified in Scheme 1.

If indeed the mechanistic similarities between methanol and halomethane conversion are as profound as suggested above, the main difference must be the addition of C_1 entities to the hydrocarbon pool, that is, methylation steps. Dealkylation steps should be independent of the original reactant. In this report we present a description of the methylation of ethene, propene,[29] and toluene by chloromethane, bromomethane, and iodomethane, using quantum chemical methods. A 19 atom cluster model containing four tetrahedral atoms (denoted 4T) has been used to represent the zeolite catalyst. Within the cluster approach, a small fragment is used to simulate the Brönsted acidic site. Calculations with such clusters have shown them to be sufficient to qualitatively describe chemical rearrangements that occur locally on the active site.[30] Structure specific effects and effects caused by the electrostatic field present in the zeolite micropores are, however, not well described. The cluster employed in this work has been used by several workers to model reactions similar to those described here.[31−37] Rozanska[31,33] et al. have studied the isomerization and transalkylation of toluene and xylenes and found that the relative order of activation energies is conserved when comparing results from cluster studies with calculations relying on periodical boundary conditions combined with plane wave basis sets. Also, alkylation of arenes[32,34,36] and alkenes[37] by methanol and reactions of sulfur containing compounds[35] have been successfully investigated using the 4T atom cluster.

Adsorbed reactants, transition states, and adsorbed products have been optimized, and both the associative (direct) and dissociative (via the formation of framework methoxide groups) methylation mechanisms have been examined. In total, 15 reaction steps, encompassing 45 stationary points, have thus been modeled. The order of reactivity among the halomethanes has been assessed, and comparison with recent relevant theoretical work on methanol reactivity[31−37] has been made. No attempts have been made to describe initial formation of C−C bonds. This reaction step has been claimed to be of little importance for methanol conversion,[38] as it is clear that the hydrocarbon pool mechanism prevails once a reasonable amount of hydrocarbon adsorbate has been built up inside the zeolite pores. We expect this argument to be valid for halomethane conversion as well.

2. Computational Details

All calculations were done using the Gaussian98 program package.[39] The B3LYP hybrid density functional was employed for all geometry optimizations. No geometric constraints were used in the optimizations. The 6-31G(d) basis sets incorporated in the Gaussian98 program were applied for hydrogen, oxygen, carbon, aluminum, and silicon. LANL2DZdp effective core potentials[40,41] (ECPs) were used on chlorine, bromine, and iodine. Additionally, single-point electronic energies were calculated for the optimized geometries using MP2 and basis sets as above. Single-point calculations were also carried out using B3LYP and the full 6-311G(d,p) basis sets (no ECPs). The 6-311G(d,p) basis set for iodine was taken from ref 42. All basis sets not included in Gaussian98 were obtained from the EMSL Web site.[43] The ultrafine integration grid was used for geometry optimizations in order to ensure convergence. B3LYP_ECP and MP2_ECP will in the following be used as acronyms to indicate when ECPs have been used.

The zeolite catalyst has been modeled using a cluster consisting of four tetrahedral atoms, that is, three silicon atoms and one aluminum atom, to generate the acidic site.[36,37] To reduce the effect of using a finite cluster model, care was taken to ensure that reactants and products were coordinated similarly to the cluster for all reactions. For all stationary points, vibrational spectra were calculated to ensure that the correct number of imaginary frequencies was at hand, that is, one imaginary frequency for transition states and zero for energy minima. For the transition states, the normal modes corresponding to the imaginary frequencies were visualized to confirm that they indeed corresponded to the expected motion of atoms. Internal reaction coordinate (IRC) calculations, as implemented in Gaussian98, were in some cases carried out. Such calculations follow reaction paths in order to investigate the minima connected by the transition states. A step size of 0.3 $amu^{-1/2}$ bohr and the ultrafine integration grid were used.

3. Results and Discussion

Methylation of ethene, propene, and toluene has been chosen as model reactions to probe the relative reactivity of chloromethane, bromomethane, and iodomethane over acidic zeolite catalysts. The reactions result in formation of propene (from ethene), *trans*-2-butene (from propene), and *p*-xylene (from toluene) together with a hydrogen halide molecule. The other possibilities, resulting in *cis*-2-butene from propene and *m*- or *o*-xylene from toluene, have not been investigated. Adsorption modes, transition barriers, and the reaction products have been analyzed, both energetically and geometrically. Recent theoretical reports on methylation of alkenes[37] and methylbenzenes[36] with methanol describe the formation of charged hydrocarbon species as shallow energy minima on the potential energy surface (PES) in the presence of water. A test calculation was performed for the methylation of propene by chloromethane, and a stationary point (without imaginary frequencies) describing an adsorbed charged hydrocarbon species was found also in this case. The hydrocarbon fragment was bridged, similar to methyl substituted protonated cyclopropane, as has been observed previously.[37] However, the coordination of the hydrocarbon species to the cluster was somewhat unsatisfying in the sense that the hydrogen atoms available for return to the catalyst were oriented away from the zeolite oxygen atoms and into vacuum. Further, the barrier for reorientation and deprotonation is expected to be very low. Nonetheless, it seems fairly clear that methylation reactions have to proceed via geometries closely resembling carbocations, whether these are stationary points or not.[37]

Two different likely mechanistic pathways have been investigated: The associative mechanism, which is described in subsection 3.1, and the dissociative mechanism, described in subsection 3.2. In the following, when energies are discussed,

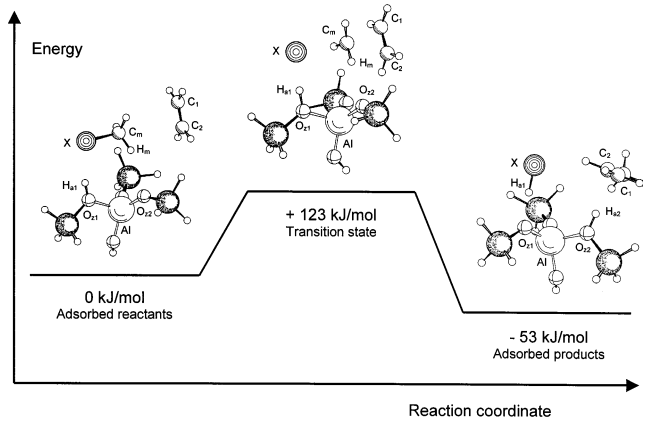

Figure 1. Stationary points along the reaction path for associative methylation of ethene by chloromethane.

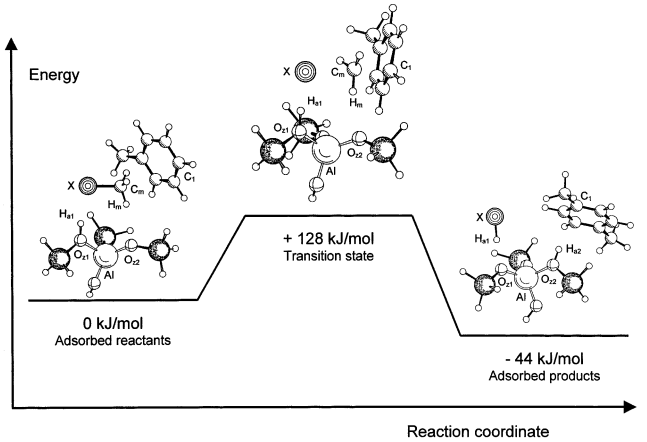

Figure 2. Stationary points along the reaction path for associative methylation of toluene by chloromethane.

we refer to the B3LYP_ECP/6-31G(d) + ZPE values, unless otherwise stated.

3.1. Associative Methylation. In this pathway, the halomethane and hydrocarbon reactant are initially coadsorbed on the cluster. In a single reaction step, the methyl group is transferred from the halomethane to the hydrocarbon and a hydrogen halide is formed. The resulting product hydrocarbon (with one more C-atom than the reactant) and the hydrogen halide molecule are then coadsorbed. Figure 1 shows the stationary points for the associative methylation of ethene by chloromethane, and Figure 2 displays the same information for methylation of toluene by chloromethane. Energies and geometric parameters related to associative methylation are listed in Tables 1 and 2, respectively.

3.1.1. Adsorbed Reactants. The energetically most favored adsorption mode for the halomethanes can be labeled as side-on adsorption, as can be seen in Figure 1. The large diffuse electron cloud of the halogen atom is associated with the acidic proton of the zeolite model. The $O_{z1}H_{a1}$ bond is slightly stretched, from 0.97 Å for the free cluster model to 0.98 Å upon coordination of a halomethane to the acidic site. The $H_{a1}X$ distance depends on halogen size, and increasing the halogen atom size also causes the halomethane methyl carbon to be lifted up from the cluster, as can be seen from the C_mAl distances. One of the hydrogen atoms of the methyl group is coordinated to a zeolite oxygen atom. This weak interaction is indicated by the H_mO_{z2} distances in Table 2. The side-on adsorption causes the XC_m bonds to be stretched by 0.01−0.03 Å, relative to the bond lengths calculated in the gas phase. Adsorption of chloromethane on zeolite acid sites has been examined previously by Su and Jaumain,[45] using FT-IR spectroscopy. They found that the interaction between the chlorine and the acidic proton caused the zeolite hydroxyl to be stretched sufficiently to cause a measurable shift in the IR frequency, which correlates well with the calculated increase in bond length reported here. No discussion on the side-on nature of the adsorption was given by Su and Jaumain.[45]

The double bonds of ethene and propene are coordinated to the methyl carbon atom of the halomethane and to the cluster itself. The XC_m axis is directed toward the double bond, and the four atoms are all in the same plane, as can clearly be seen from the $XC_1C_2C_m$ dihedral angles. Toluene is adsorbed in a similar manner, except that the methyl groups of the halomethanes are not pointing toward any specific region of the toluene molecule; see Figure 2. Therefore, only the XC_mC_1 (C_1 is the ring carbon in the para position to the toluene methyl group) angle is given in Table 2.

The coadsorption energies are between 30 and 40 kJ/mol. A weak trend is observed; it appears that increasing the halogen atom size results in a slightly weaker interaction. Replacing ethene or propene with toluene makes the adsorption somewhat stronger. The adsorption energies are fairly modest, compared to energies close to 90 kJ/mol calculated in exactly the same manner for coadsorption of methanol and a series of different hydrocarbons on the cluster.[36,37] This means that, in experimental practice, higher partial pressures must be applied for the halomethanes than for methanol in order to reach the same degree of surface coverage. All adsorption energies become considerably larger when the MP2 level of theory is used. This has also been observed in the previous studies on methanol reactivity,[36,37] and it can be ascribed to the superior description of long-range van der Waals interactions by the MP2 scheme compared to the B3LYP methodology.[46]

3.1.2. Transition States and Activation Barriers. In the transition states, the XC_m bond is lengthened and the methyl group is moving from the halogen toward the hydrocarbon to be methylated. Umbrella-like inversion of the formal CH_3^+ group has proceeded beyond the planar inversion point. This is evident from the methyl dihedral angles in Table 2. Very significantly, the halomethanes are not protonated. However, the $O_{z1}H_{a1}$ bonds are considerably stretched, and the $H_{a1}X$ distances correspondingly shortened, but no complete proton transfer has occurred. An IRC calculation was performed for the methylation of propene by chloromethane, and this confirmed that the correct transition state had been found. The IRC calculation also revealed that the acidic proton is transferred from the zeolite oxygen to the halogen after the bond between the hydrocarbon and the methyl cation is formed.

For ethene, it appears that the methyl cation is approaching the center of the double bond in a three-ring arrangement, which is indicated by the almost identical distances from C_m to the carbon atoms of the double bond. This nearly symmetrical coordination has been described previously in a similar cluster study in which methanol was the methylating agent.[37] It was then concluded that the reaction pathway from the transition state down to propene proceeds via a protonated cyclopropane, which undergoes a single-step isomerization to form a secondary propyl cation. Deprotonation then yields propene. The similarities between the mechanistic details disclosed here and those described for the methanol reactions are so profound that this conclusion must also be valid when a halomethane is reacting with ethene. For propene, the C_mC_1 and C_mC_2 distances are quite different, and it seems that the methyl cation is being attached

TABLE 1: Energies of Stationary Points for Associative Methylation Reactions and Gas-Phase Reaction Energies[a]

	energy of						
	gas-phase reactant	transition state	adsorbed products	gas-phase products	gas-phase reaction energy	calc gas-phase reaction enthalpy	exp gas-phase reaction enthalpy[b]
				B3LYP_ECP/6-31G(d) + ZPE			
ethene +							
chloromethane	35	123	−53	7	−28	−27	−41
bromomethane	34	118	−43	12	−22	−21	−34
iodomethane	31	117	−32	14	−17	−17	−20
propene +							
chloromethane	36	108	−51	9	−27	−25	−40
bromomethane	35	101	−40	14	−21	−19	−33
iodomethane	31	97	−30	15	−17	−15	−19
toluene +							
chloromethane	39	128	−44	13	−25	−22	−41
bromomethane	38	120	−33	18	−19	−16	−34
iodomethane	34	115	−23	19	−15	−12	−20
				B3LYP_ECP/6-31G(d)			
ethene +							
chloromethane	42	124	−50	21	−21		
bromomethane	41	118	−39	26	−15		
iodomethane	37	116	−28	27	−10		
propene +							
chloromethane	42	110	−48	23	−19		
bromomethane	41	102	−37	28	−13		
iodomethane	37	97	−25	30	−8		
toluene +							
chloromethane	47	133	−35	32	−15		
bromomethane	45	123	−24	36	−9		
iodomethane	41	116	−14	37	−4		
				B3LYP/6-311G(d,p)// B3LYP_ECP/6-31G(d)			
ethene +							
chloromethane	35	126	−62	2	−34		
bromomethane	35	122	−48	11	−24		
iodomethane	35	125	−30	19	−17		
propene +							
chloromethane	37	115	−59	5	−31		
bromomethane	35	109	−42	14	−22		
iodomethane	33	100	−29	19	−14		
toluene +							
chloromethane	32	129	−53	6	−27		
bromomethane	40	130	−29	23	−17		
iodomethane	34	118	−18	24	−9		
				MP2_ECP/6-31G(d)// B3LYP_ECP/6-31G(d)			
ethene +							
chloromethane	56	138	−58	30	−26		
bromomethane	55	125	−47	37	−18		
iodomethane	50	117	−35	39	−11		
propene +							
chloromethane	59	129	−59	33	−26		
bromomethane	59	124	−46	41	−18		
iodomethane	55	118	−34	44	−11		
toluene +							
chloromethane	68	161	−53	41	−27		
bromomethane	67	148	−41	48	−19		
iodomethane	60	135	−35	49	−12		

[a] All values are relative to the adsorbed reactants and are in kJ/mol. Enthalpies are at 298 K. [b] Experimentally determined gas-phase reaction enthalpies taken from ref 44.

to the least substituted carbon atom of the double bond and that a secondary butyl cation is formed, which agrees well with the expected outcome of an electrophilic substitution reaction. Subsequent deprotonation results in formation of 2-butene. When toluene is methylated, there is no three-ring arrangement. A bond is formed directly between the methyl cation and the carbon atom in the para position to the toluene methyl group. The XC_mC_1 angles, which are nearly 180°, are reported in Table 2. This is again analogous to the geometry of the transition state for methylbenzene methylation with methanol.[32,34,36]

The barrier height and the geometry of the transition state may be expected to depend on both the nature of the halogen atom and the nature of the hydrocarbon. On the basis of the activation energies, listed in column 2 of Table 1, two issues merit further discussion. First, propene is more easily methylated than ethene, and toluene is predicted to have a reactivity similar to that of ethene. The same order has been observed in similar studies with methanol as methylating agent.[36,37] The higher reactivity of propene with respect to ethene found both here and in the literature may be rationalized by considering the cation expected to form immediately after the transition state. For ethene, highly unstable protonated cyclopropane is formed, while an energetically favored secondary butyl cation is formed after the methylation of propene, and the barrier is accordingly

TABLE 2: Geometric Parameters for Associative Methylation[a]

	ethene +			propene +			toluene +		
	MeCl	MeBr	MeI	MeCl	MeBr	MeI	MeCl	MeBr	MeI
adsorbed reactants									
$O_{z1}H_{a1}$	0.98	0.98	0.98	0.98	0.98	0.98	0.98	0.98	0.98
$H_{a1}X$	2.25	2.41	2.63	2.25	2.41	2.63	2.23	2.39	2.62
XC_m[b]	1.83	1.99	2.18	1.83	1.99	2.18	1.83	1.99	2.18
XAl	4.34	4.50	4.69	4.34	4.51	4.68	4.44	4.59	4.75
C_mAl	4.12	4.17	4.23	4.10	4.18	4.22	4.37	4.41	4.41
C_mC_1[c]	3.60	3.62	3.66	3.60	3.62	3.69	3.86	3.86	3.87
C_mC_2[c]	3.68	3.69	3.75	3.70	3.63	3.67			
C_1C_2	1.33	1.33	1.33	1.34	1.34	1.34			
H_mO_{z2}	2.47	2.46	2.47	2.46	2.44	2.47	2.44	2.43	2.45
$O_{z1}H_{a1}X$	167.0	167.8	166.5	166.8	167.7	165.9	171.0	171.1	169.8
$XC_1C_2C_m$	1.1	1.1	1.5	2.6	2.6	3.5			
XC_mC_1							147.5	148.6	147.6
dihedral methyl[d]	31.9	31.2	31.2	31.9	31.2	31.2	31.7	31.1	30.9
transition states									
$O_{z1}H_{a1}$	1.03	1.03	1.02	1.03	1.02	1.01	1.03	1.02	1.01
$H_{a1}X$	1.90	2.09	2.33	1.93	2.14	2.40	1.93	2.14	2.39
XC_m	2.67	2.86	3.08	2.60	2.76	2.93	2.65	2.80	2.98
XAl	4.08	4.27	4.49	4.14	4.37	4.60	4.22	4.42	4.65
C_mAl	3.71	3.76	3.81	3.66	3.71	3.78	4.05	4.12	4.20
C_mC_1[c]	2.08	2.06	2.04	2.05	1.99	1.99	1.94	1.93	1.94
C_mC_2[c]	2.09	2.07	2.06	2.31	2.41	2.49			
C_1C_2	1.36	1.36	1.37	1.37	1.37	1.37			
H_mO_{z2}	2.21	2.21	2.22	2.30	2.33	2.35	2.24	2.27	2.31
$O_{z1}H_{a1}X$	174.7	175.2	175.5	174.8	175.2	174.6	177.5	177.8	177.4
$XC_1C_2C_m$	2.4	2.6	2.8	2.3	2.9	2.9			
XC_mC_1							175.1	175.3	175.6
dihedral methyl	−19.6	−21.5	−22.9	−16.1	−16.9	−16.5	−18.7	−19.2	−19.0
imaginary frequency of TS	327i	316i	313i	341i	336i	359i	354i	354i	367i
adsorbed products									
$O_{z1}H_{a1}$	1.69	1.71	1.80	1.70	1.72	1.83	1.71	1.73	1.84
$H_{a1}X$	1.33	1.49	1.67	1.33	1.49	1.66	1.33	1.49	1.66
XC_m	5.20	5.37	5.59	4.32	4.53	4.92	4.42	4.68	6.02
XAl	4.04	4.22	4.49	4.09	4.26	4.53	4.06	4.25	4.49
$H_{a2}C_1$[e]	2.13	2.14	2.15	2.15	2.15	2.21			
$H_{a2}C_2$[e]	2.27	2.27	2.27	2.20	2.20	2.17			
$O_{z2}H_{a2}$	0.99	0.99	0.99	0.99	0.99	0.99	0.99	0.99	0.99
$H_{a2}C_3$[f]							2.20	2.21	2.14
$H_{a2}C_4$[f]							2.32	2.32	2.44
C_3C_4							1.40	1.40	1.40
C_1C_2	1.34	1.34	1.34	1.35	1.35	1.34			
$O_{z1}H_{a1}X$	175.1	176.1	176.7	175.9	176.7	176.9	175.4	176.0	176.6
$O_{z2}C_1C_2H_{a2}$	0.6	0.6	0.9	0.8	0.7	0.9	2.3	2.2	1.9

[a] Distances in Å; angles in deg; frequencies in cm^{-1}. Atom labels are defined in Figures 1 and 2. [b] The calculated gas-phase XC_m distances are 1.80 Å for MeCl, 1.98 Å for MeBr, and 2.17 Å for MeI. [c] For propene, C_1 is the hydrogen substituted carbon and C_2 is the methyl substituted carbon of the double bond. [d] This is the dihedral angle defined by the four atoms of the halomethane methyl group, HHHC. It describes the degree of inversion of the methyl group. [e] For propene, formed from ethene, C_2 is the methyl substituted carbon of the double bond. [f] For *p*-xylene, formed from toluene, C_3 and C_4 are two hydrogen substituted ring carbons. The acidic proton is coordinated to the C_3C_4 bond.

lower. This is also reflected in a shift in geometry toward a more reactant-like transition state for the methylation of propene, as predicted from the Hammond postulate.[47] The fairly high activation barrier for toluene cannot be as easily rationalized. It might be speculated that the partial localization of aromatic electrons in the transition state causes the barrier to be relatively high, as some aromaticity is lost.

Second, the barriers for methylation by iodomethane are somewhat lower (by 1−5 kJ/mol) than those for methylation by bromomethane, which in turn are lower (by 5−8 kJ/mol) than those for chloromethane. This same trend was observed for all three hydrocarbon reactants and at every level of theory employed, apart from two minor exceptions, found when the B3LYP/6-311G(d,p)//B3LYP_ECP/6-31G(d) methodology was used. First, for methylation of ethene, the reactivity of bromomethane is shifted above that of iodomethane, but the difference between the barriers for all three halomethanes is only 4 kJ/mol. Second, for the methylation of toluene, the reactivities of chloromethane and bromomethane are predicted to be equal within 1 kJ/mol. Drawing definitive conclusions on the order of reactivity among the halomethanes on the basis of these small differences may not be warranted. Both the polarizabilities and dipole moments of the three halomethanes are different, and the expected downward shift in barrier height upon inclusion of the electrostatic field present in a real zeolite catalyst might not be uniform. The calculated trend does, however, conform with the order of reactivity determined experimentally when alkali-exchanged zeolites were employed.[24] Notably, there is a substantial increase in the barrier height for methylation of toluene calculated at the MP2_ECP/6-31G(d)// B3LYP_ECP/6-31G(d) level of theory, by 20−30 kJ/mol, relative to the value at the B3LYP_ECP/6-31G(d) + ZPE level. This shifts the barrier for toluene methylation well above the barrier for ethene methylation and illustrates that quantitative assessments of the results should be made cautiously.

From the geometric parameters for the transition states listed in Table 2, some effects of the halogen atom type may be discerned, and it is possible to correlate the small differences

in activation barriers with geometric trends. A lower barrier height again implicates that the reaction has passed a shorter distance along the reaction coordinate at the transition state, and the geometry should to a greater degree resemble that of the reactants. This is in part observed. The $O_{z1}H_{a1}$ bond length decreases when the barrier increases. Similar theoretical studies of the methylation of propene with methanol, where methanol is protonated in the transition state, have shown that the activation energy is linked to the ease of removal of the acidic proton from the catalyst model.[37] In the methanol case, it seems reasonable to assume that a major contribution to the barrier lies in the breaking of the $O_{z1}H_{a1}$ bond in the protonation and the resulting separation of charges. When halomethanes are the methylating agent, there is no complete protonation, but it can be concluded that, for iodine, the XC_m bond is sufficiently activated with only a moderate stretch of the $O_{z1}H_{a1}$ bond. For bromine, and especially chlorine, a stronger interaction with the acidic proton is required for XC_m activation. The proton is therefore removed further from the cluster, and the activation energy is accordingly higher.

There is no detectable systematic trend in the distances from the methyl cation to the hydrocarbon (C_mC_1 and C_mC_2) when going form chloromethane to bromomethane to iodomethane.

3.1.3. Adsorbed Products and Reaction Energies. The reaction products, a hydrogen halide molecule and a hydrocarbon with one more carbon atom than the reactant, are also coadsorbed on the cluster. The hydrocarbon is adsorbed on the acidic site, while the hydrogen halide is adsorbed end on and forms a hydrogen bond to one of the zeolite oxygen atoms. The $O_{z1}H_{a1}$ distance, which describes this hydrogen bond, is in every case shortest for hydrogen chloride and longest for hydrogen iodide, opposite of what might be expected on the basis of the differences in acid strength. Hydrogen iodide is the strongest acid, in the gas phase, both experimentally and at the B3LYP_ECP/6-31G(d) + ZPE level of theory.[48] Increasing halogen atom size might also result in an increase in the steric repulsion between the halogen and the cluster, and this could explain the observed trend in the $O_{z1}H_{a1}$ distances. Indeed, the sum of the $O_{z1}H_{a1}$ and $H_{a1}X$ distances is in every case about 0.2 Å shorter than the sum of the ionic radii of oxygen and the relevant halogen.

The coadsorption energies of the products are larger than those for the reactants, and this causes the cluster reaction energies to be more exothermic than the gas-phase reaction energies. For the products, there are two factors that mainly contribute to the adsorption energy: the hydrogen halide associated to the zeolite oxygen and the acidic proton coordinated to the electrons of the hydrocarbon double bond. This compares to one such interaction for the reactants, that is, the halogen atom coordinated to the acidic site. On the basis of the number of proper interactions between adsorbate and adsorbent, it is then fairly easy to explain the stronger adsorption of the products relative to the reactants.

The trend in experimental gas-phase reaction enthalpies, listed in column 7 of Table 1, is nicely reproduced by the calculations, both in the adsorbed state and in the gas phase. The levels of theory employed are, however, not sufficient to quantitatively reproduce the experimental reaction enthalpies.

3.2. Dissociative Methylation. In the dissociative mechanism, the halomethane is first adsorbed alone on the cluster. Then, in a single step, the halomethane dissociates as the methyl group is transferred to a zeolitic oxygen, and a hydrogen halide and a framework bonded methoxide are formed. Later on, the hydrogen halide is displaced by a hydrocarbon, to which the framework methyl group is transferred in an activated reaction step. The net overall reaction is the same as that for the associative mechanism. Figures 3 and 4 depict the stationary points for the formation of surface methoxide from chloromethane and methylation of ethene by the methoxide species, respectively. Energies and geometric parameters for methoxide formation are listed in Tables 3 and 4, and energies and geometric details for methylations with the surface methoxide will be found in Tables 5 and 6.

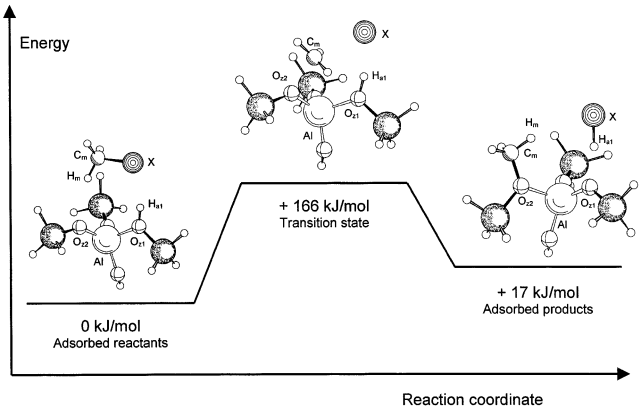

Figure 3. Stationary points along the reaction path for the formation of a surface methoxide from chloromethane.

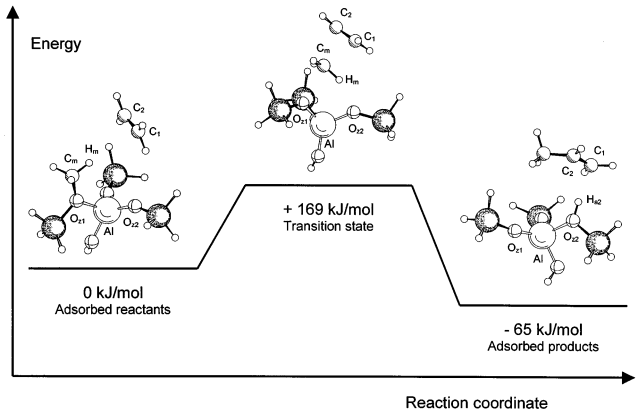

Figure 4. Stationary points along the reaction path for the methylation of ethene by a surface methoxide.

3.2.1. Formation of Zeolite Bonded Methoxide Groups. The adsorption modes of the halomethanes appear to be virtually independent of the presence of a coadsorbate. Side-on adsorption, with the halogen atom coordinated to the acidic site and one of the hydrogen atoms of the methyl group in interaction with a zeolite oxygen atom, is again favored. The distances describing the adsorbed halomethanes, listed in Table 4, are very nearly identical to those found in Table 2 for the halomethanes with a coadsorbate present. As can be seen from the first column of Table 3, the adsorption energies are similar for all halomethanes, only a slightly smaller energy is found when the atomic number of the halogen increases. The same trend was found for the coadsorption energies described in subsection 3.1.1. The difference between the adsorption energy of a halomethane alone and the adsorption energy found when the halomethane and a hydrocarbon are coadsorbed should be a measure of the strength of the binding of the hydrocarbon in the coadsorption mode. A comparison of the energies listed in column 1 of Table 1 and column 1 of Table 3 reveals that the B3LYP functional with the employed basis sets inadequately describes this weak adsorption. There is no substantial difference in the adsorption energies found with or without a hydrocarbon

TABLE 3: Energies of Stationary Points for Formation of Methoxide and Adsorbed Hydrogen Halide[a]

	energy of		
	gas-phase reactant	transition state	adsorbed products
B3LYP_ECP/6-31G(d) + ZPE			
chloromethane	32	166	17
bromomethane	31	155	27
iodomethane	28	149	37
B3LYP_ECP/6-31G(d)			
chloromethane	36	168	20
bromomethane	35	156	31
iodomethane	32	149	43
B3LYP/6-311G(d,p)// B3LYP_ECP/6-31G(d)			
chloromethane	35	170	24
bromomethane	36	159	42
iodomethane	34	150	54
MP2_ECP/6-31G(d)// B3LYP_ECP/6-31G(d)			
chloromethane	45	198	21
bromomethane	44	181	33
iodomethane	40	169	45

[a] All values are relative to the adsorbed halomethane and are in kJ/mol.

TABLE 4: Geometric Parameters for the Formation of a Surface Methoxide Species and a Hydrogen Halide Molecule from Chloromethane, Bromomethane, and Iodomethane[a]

	MeCl	MeBr	MeI
adsorbed reactants			
$O_{z1}H_{a1}$	0.98	0.98	0.98
$H_{a1}X$	2.26	2.42	2.65
XC_m	1.82	1.99	2.18
XAl	4.34	4.48	4.67
C_mAl	4.12	4.14	4.20
H_mO_{z2}	2.39	2.39	2.40
C_mO_{z2}	3.45	3.45	3.47
$O_{z1}H_{a1}X$	166.2	166.3	165.0
XC_mO_{z2}	98.4	99.6	99.6
dihedral methyl[b]	31.8	31.2	31.1
transition states			
$O_{z1}H_{a1}$	1.01	1.01	1.01
$H_{a1}X$	2.12	2.31	2.57
XC_m	2.47	2.64	2.85
C_mO_{z2}	1.93	1.92	1.91
XAl	4.35	4.53	4.76
C_mAl	2.88	2.89	2.91
$O_{z1}H_{a1}X$	163.6	163.2	162.3
XC_mO_{z2}	146.0	147.1	148.5
dihedral methyl	−7.6	−9.0	−10.3
imaginary frequency of TS	494i	475i	462i
adsorbed products			
$O_{z1}H_{a1}$	1.73	1.76	1.88
$H_{a1}X$	1.33	1.48	1.66
XC_m	3.93	4.12	4.42
H_mX	2.87	3.05	3.38
$O_{z2}C_m$	1.46	1.46	1.45
XAl	4.04	4.22	4.51
C_mAl	2.96	2.96	2.96
C_mH_mX	164.2	165.7	160.4
$O_{z1}H_{a1}X$	172.6	173.4	173.6
dihedral methyl	−34.2	−34.2	−34.3

[a] Distances in Å; angles and dihedral angles in deg; frequencies in cm^{-1}. Atom labels are defined in Figure 3. [b] This is the dihedral angle defined by the four atoms of the halomethane methyl group, HHHC.

coadsorbate. At the MP2 level of theory, however, a difference was found, indicating that the interaction energies between the hydrocarbons and the cluster are in the range 10−20 kJ/mol, depending on hydrocarbon size.

The transition states for surface methoxide formation are qualitatively quite similar to those found for the associative

TABLE 5: Energies of Stationary Points for Methylation of Ethene, Propene, and Toluene by a Zeolite Framework Methoxide Species[a]

	energy of		
	gas-phase reactant	transition state	adsorbed product
B3LYP_ECP/6-31G(d) + ZPE			
ethene	5	169	−65
propene	5	156	−63
toluene	8	171	−59
B3LYP_ECP/6-31G(d)			
ethene	7	173	−65
propene	8	162	−63
toluene	11	179	−55
B3LYP/6-311G(d,p)//B3LYP_ECP/6-31G(d)			
ethene	6	171	−78
propene	6	158	−77
toluene	6	172	−68
MP2_ECP/6-31G(d)//B3LYP_ECP/6-31G(d)			
ethene	15	181	−74
propene	17	171	−75
toluene	26	190	−75

[a] All values are relative to the energies of the hydrocarbons to be methylated adsorbed on the methoxide substituted cluster and are in kJ/mol.

TABLE 6: Geometric Parameters for Methylation of Ethene, Propene, and Toluene by a Surface Methoxide Species[a]

	ethene	propene	toluene
adsorbed reactants			
$O_{z1}C_m$	1.45	1.45	1.45
C_mC_1[b]	3.97	4.02	3.84
C_mC_2[b]	4.13	4.01	
C_1C_2	1.33	1.34	
C_mAl	3.00	3.00	2.97
$O_{z1}C_mC_1$			133.0
$O_{z1}C_1C_2H_m$	16.2	15.7	
$C_mC_1C_1H_m$	1.5	1.8	
dihedral methyl[c]	34.5	34.5	34.3
transition states			
$O_{z1}C_m$	2.25	2.22	2.25
C_mC_1	2.11	2.07	2.02
C_mC_2	2.15	2.29	
C_1C_2	1.36	1.36	
C_mAl	3.22	3.21	3.12
H_mO_{z2}	1.93	1.98	2.42
$O_{z1}C_1C_2H_m$	3.0	2.0	
$O_{z1}C_mC_1$			173.9
dihedral methyl	−15.4	−14.1	−15.6
imaginary frequency of TS	384i	380i	405i
adsorbed products			
$O_{z2}H_{a2}$	0.99	0.99	0.98
$H_{a2}C_1$[d]	2.14	2.19	
$H_{a2}C_2$[d]	2.31	2.21	
C_1C_2	1.34	1.34	
$O_{z2}C_1C_2H_{a2}$	3.1	3.0	
$H_{a2}C_3$[e]			2.30
$H_{a2}C_4$[e]			2.33
C_3C_4			1.40
$O_{z2}C_3C_4H_{a2}$			0.6

[a] Distances in Å; angles and dihedral angles in deg; frequencies in cm^{-1}. Atom labels are defined in Figures 4 and 2. [b] For propene, C_1 is the hydrogen substituted carbon and C_2 is the methyl substituted carbon of the double bond. [c] This is the dihedral angle defined by the four atoms of the halomethane methyl group, HHHC. [d] For propene, formed from ethene, C_2 is the methyl substituted carbon of the double bond. [e] For *p*-xylene, formed from toluene, C_3 and C_4 are two hydrogen substituted ring carbons. The acidic proton is coordinated to the C_3C_4 bond.

methylation, described above. The methyl cation is about halfway between the halogen atom and one of the zeolite oxygen

atoms. The halogen does clearly interact with the acidic site, but there is no complete protonation. IRC calculations showed that a bond was formed between the methyl cation and the zeolite oxygen before the acidic proton was completely transferred to the halogen. The normal mode of the transition state is defined by X, C_m, and O_{z2}, and as indicated by the XC_mO_{z2} angles, there is considerable deviation from linearity. In fact, the transition state may be considered to be a six-ring arrangement of the involved atoms ($XC_mO_{z2}AlO_{z1}H_{a1}$).

The activation barriers for methoxide formation follow the same trend as was found for associative methylation, that is, the highest barrier is found for chloromethane and the lowest for iodomethane. The differences are somewhat more pronounced than previously, and they are largest at the MP2_ECP/6-31G(d)//B3LYP_ECP/6-31G(d) level of theory. The activation energies found are, however, substantially higher than those found for associative methylation, at every level of theory used. Notably, at the MP2_ECP/6-31G(d)//B3LYP_ECP/6-31G(d) level of theory, there is a considerable increase in the calculated barriers.

Both the XC_m and $O_{z1}H_{a1}$ distances are shorter than what was found in the case of associative methylation. Also, the degree of inversion of the methyl cation is considerably less pronounced. This illustrates how dissociation of the halomethane molecule has proceeded further at the transition state for associative methylation than in the case for methoxide formation. Formation of the surface methoxide and a hydrogen halide molecule is an endothermic reaction. The trend in reaction energy among the different halomethanes is the same as that for associative methylation; the reaction is thermodynamically less unfavorable for chloromethane than for bromomethane and iodomethane.

3.2.2. Methylation by the Methoxide Species. Because of the limited size of the cluster model employed in this study, the further progress of the dissociative reaction mechanism has to proceed via the displacement of the hydrogen halide into the gas phase and adsorption of the hydrocarbon reactant onto the cluster with the methoxide group. As depicted in Figure 4, for ethene and propene, the hydrocarbon is partly coordinated to the cluster itself, as well as to the methoxide group. The C_mH_m axis is clearly pointing directly at the alkene double bond, and the $C_mC_1C_2H_m$ dihedral angle is nearly zero, showing that the four atoms are in the same plane. For toluene, the adsorption mode is similar, but the interaction between the methoxide hydrogen (H_m) and the π-system is less obvious. This is the same arrangement as reported for benzene adsorption on a cluster with a methoxide group.[31,33,34] A second, distinctively different adsorption mode also exists, where the hydrocarbon is located directly above the methoxide group, and the π-electrons of the hydrocarbons are coordinated to C_m and not to H_m. For the alkenes, the $O_{z1}C_1C_1C_m$ dihedral angles are then very nearly zero. Energetically, these two possibilities are indistinguishable, and it turns out that adding the ZPE corrections to the electronic energies (B3LYP_ECP/6-31G(d)) in one case reverses the order of stability of the two arrangements. The adsorption mode presented here has been selected because it to the greatest degree resembles previously published results on similar reactions.[31,33,34] Selecting the on-top starting point for the reactions would not result in any change in the activation or reaction energies presented here, nor would it affect any predictions on relative reactivities.

The calculated adsorption energies (column 1 of Table 5) are very small when the B3LYP functional is used, but the predicted strength of the interaction increases considerably when

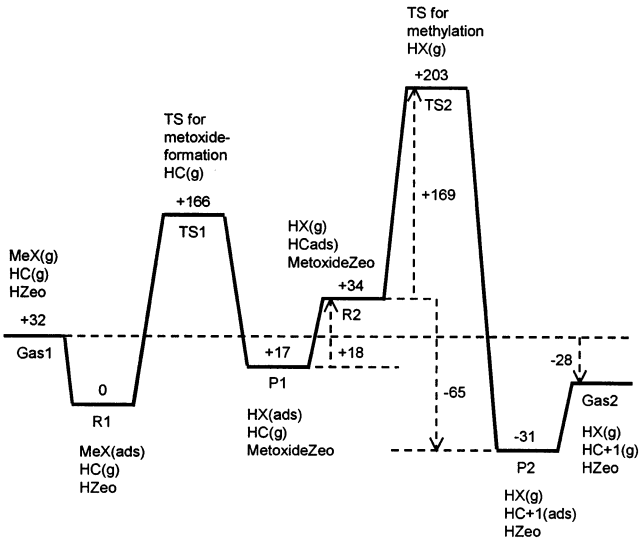

Figure 5. Energy diagram for the complete reaction pathway of dissociative methylation. The energy difference between P1 and R2 corresponds to the difference in adsorption energy between the hydrogen halide and the hydrocarbon. This step in energy may be considered an effect of the limited cluster size. MeX = halomethane, HC = hydrocarbon, HZeo = protonated cluster, HX = hydrogen halide, MethoxideZeo = methoxide substituted cluster, HC+1 = methylated hydrocarbon. Energies correspond to methylation of ethene by chloromethane, in kJ/mol.

MP2 is used. At the MP2 level it is also possible to order the adsorption energies of the three hydrocarbons: The larger the hydrocarbon, the stronger is the adsorption. This is closely related to the assessment of the strength of the interaction between a hydrocarbon and a cluster with a halomethane already coordinated to the acidic site, as discussed above. It is clear that the energetically dominating part of any adsorption on the cluster involves coordination to the acidic site.

The transition states for methylation from the methoxide species described here closely resemble that reported for methylation of benzene, also by a methoxide species.[31,33,34] The methoxide leaves the zeolite oxygen as a methyl cation, which is moving toward the hydrocarbon. Inversion of the methyl cation has not fully progressed to the planar inversion point. In a manner similar to the associative methylation described above, the methyl cation is coordinated to the center of the alkene double bonds. For ethene, the progress of the reaction is again expected to involve formation of a protonated cyclopropane, which is isomerized into a secondary propyl cation. The order of reactivity among the hydrocarbons is the same as that for the associative step, and the same argumentation can be used to rationalize the results. All calculated barriers are, however, significantly higher than those in the associative case.

At the end point of the reaction pathway for the dissociative methylation, the hydrocarbon with one more carbon atom than the initial reactant is adsorbed onto the acidic site, as displayed in Figure 4. These stationary points are basically identical to those described for the adsorbed products after associative methylation, except that no hydrogen halide is present.

3.3. Implications for Catalysis and Comparison with Methanol Conversion. Figure 5 displays how the results from the two steps of the dissociative mechanism can be connected to describe the entire reaction path. We have studied nine different total reactions; each hydrocarbon can react with each halomethane. It is very clear that the associative pathway is favored over the dissociative one. Both barriers of the dissociative mechanism are higher than the single barrier of the

associative pathway. Xia et al.[49] have investigated the mechanism of chloromethane conversion over H-ZSM-5 using in situ FTIR spectroscopy, and they proposed a mechanism involving surface methoxide and alkoxide groups as important intermediates. Methoxide formation from halomethanes on acidic zeolites has also been observed experimentally by others.[19,24,50−52] The predicted barriers for both formation and further reactions of the methoxide group presented here are certainly not prohibitively high and therefore do not definitively rule out reactions involving such species, but the quantum chemical analysis strongly favors the associative mechanism. We speculate that this pathway is less prone to detection by spectroscopy than surface methoxides, which, once formed, might have considerable lifetimes within the catalyst pores. Also, most such spectroscopic studies have focused on the initial stages of halomethane conversion,[19,24,49−52] when the concentrations of hydrocarbons available for the associative mechanism are low. Similar to what is seen in methanol conversion,[6,7] an induction period before maximum activity is reached has also been observed for halomethane conversion.[53,54] It may well be that the methoxide groups play a part in the initial buildup of hydrocarbons inside the zeolite pores (i.e. the hydrocarbon pool) and that associative methylation prevails once steady-state conversion has been reached.

The above conclusion differs from a similar theoretical analysis of the methylation of benzene by methanol via both the associative and dissociative mechanisms presented by Vos et al.[34] They found that formation of the framework bound methoxide resulted in a fairly high activation barrier of 220 kJ/mol but that the barrier for the second step of the dissociative pathway had a lower barrier, 186 kJ/mol, than the single barrier of the associative pathway, 195 kJ/mol. Further, Vos et al.[34] presented a kinetic analysis of the results, which indicated that the two-step mechanism was competitive with the single-step route at elevated temperatures (400 K). It is interesting to note that when halomethanes are precursors for the methoxide group, the order is reversed relative to methanol, and the precursors are more reactive toward hydrocarbons than the methoxides are.

The transition states for methoxide formation from halomethanes presented here are significantly different from the transition state for methoxide formation from methanol described by Vos et al.,[34] where the OC_mO_{z2} angle (corresponding to the XC_mO_{z2} angle here) is close to 180°, in contrast to angles close to 150° found here. When methanol is the reactant and the 4T cluster is employed, it seems that the energy gained by arranging the three atoms involved in the normal mode of the transition state in a linear fashion outweighs what could be gained by associating one of the protons on the methanol oxygen atom to a cluster oxygen atom. A comparable and equally important difference between the methanol[32,34,36,37] and halomethane cases can be found when comparing the transition states for direct methylation. When methanol is the methylating agent, there is a complete protonation in the transition state, whereas this is not the case for the halomethanes. This has to be kept in mind when comparing the barriers for associative methylation by methanol, which have been found to be 183 kJ/mol (ethene),[37] 169 kJ/mol (propene),[37] and 187 kJ/mol (toluene),[36] at an identical level of theory and using the same cluster as in the present work. As outlined above, the acidity of the cluster model is crucial in determining barrier height, and we have previously argued that the cluster employed does not fully mimic the acidity of a real zeolite.[37] This deficiency of the cluster approach affects the barriers for methanol reactions more severely than those for halomethanes, because the degree of protonation in the transition state is greater for methanol. Therefore, it seems reasonable to assume that the methanol activation energies are falsely shifted upward relative to those for the halomethanes. In conclusion, a comparison of the absolute barrier heights for the two types of reactants based on the cluster approach is not necessarily valid and may lead to wrong suppositions, as the mechanisms are qualitatively different. Indeed, experimental work indicates a lower activity for chloromethane conversion over acidic zeolite catalysts relative to methanol conversion at comparable conditions.[16,21]

As mentioned above, Vos et al.[34] have reported an activation barrier of 195 kJ/mol for methylation of benzene by a framework methoxide group, which is higher than the barrier for toluene reported here (171 kJ/mol). This is consistent with theoretical work by Arstad et al.,[36] who have shown that adding methyl groups to a benzene ring causes the reactivity toward methylation by methanol, that is, electrophilic aromatic substitution, to increase.

4. Conclusions

Methylation of ethene, propene, and toluene by chloromethane, bromomethane, and iodomethane has been investigated theoretically using the cluster approach. Both the associative mechanism and the dissociative mechanism have been studied. Both barriers of the dissociative pathway are higher than the single barrier of associative methylation, and the associative mechanism will be favored. This result differs from a similar comparison of the two mechanisms employing methanol as the alkylating agent.[34] It was then found that the methoxide groups, once formed, are more reactive than the original reactant.[34] Only small reactivity differences were found among the halomethanes, indicating that iodomethane is more reactive than bromomethane, which in turn is more reactive than chloromethane. Although this is in agreement with experimental results employing alkali-exchanged zeolites,[24] the differences in barriers are so small that a definitive conclusion may not be warranted. Single-point energies have been calculated at various levels of theory, and the trends presented are independent of methodology.

Acknowledgment. Thanks are due to the Norwegian Research Council for a grant of computer time through the NOTUR project (accounts NN2878K and NN2147K).

References and Notes

(1) British Petroleum statistical review of world energy June 2002. http://www.bp.com/centres/energy2002/index.asp (accessed Dec. 2002).

(2) See, for instance: *Natural Gas Conversion VI*; Iglesia, E., Spivey, J. J., Fleisch, T. H., Eds.; Stud. Surf. Sci. Catal. 136; Elsevier Science: Amsterdam, 2001.

(3) Kochloefl, K. Methane Steam Reforming. In *Handbook of Heterogeneous Catalysis, Vol 4*; Ertl, G., Knözinger, H., Weitkamp, J., Eds.; VCH Verlagsgesellschaft mbH: Weinheim, Germany, 1997; pp 1819−1831.

(4) Ponec, V. Carbon Monoxide and Carbon Dioxide Hydrogenation. In *Handbook of Heterogeneous Catalysis, Vol 4*; Ertl, G., Knözinger, H., Weitkamp, J., Eds.; VCH Verlagsgesellschaft mbH: Weinheim, Germany, 1997; pp 1876−1894.

(5) Hansen, J. B. Methanol Synthesis. In *Handbook of Heterogeneous Catalysis, Vol 4*; Ertl, G., Knözinger, H., Weitkamp, J., Eds.; VCH Verlagsgesellschaft mbH: Weinheim, Germany, 1997; pp 1856−1876.

(6) Stöcker, M. *Microporous Mesoporous Mater.* **1999**, *29*, 3−48.

(7) Chang, C. D. The Methanol-to-Hydrocarbons Reaction: A Mechanistic Perspective. In *Shape Selective Catalysis*; Song, C., Garcés, J. M., Sugi, Y., Eds.; ACS Symposium Series 738; American Chemical Society: Washington, DC, 2000; pp 96−114.

(8) (a) Noceti, R. P.; Taylor, C. E. U.S. Patent 4,769,504, Sept. 6, 1998. (b) Taylor, C. E.; Noceti, R. P. U.S. Patent 5,019,652, May 28, 1991. (c) Taylor, C. E.; Noceti, R. P. U.S. Patent 5,139,991, Aug. 18, 1992.

(9) Olah, G. A.; Gupta, B.; Farina, M.; Felberg, J. D.; Ip, W. M.; Husain, A.; Karpeles, R.; Lammertsma, K.; Melhotra, A. K.; Trivedi, N. J. *J. Am. Chem. Soc.* **1985**, *107*, 7097−7105.

(10) Butter, A. A.; Jurewicz, A. T.; Kaeding, W. W. U.S. Patent 3,-894,407, July 8, 1975.

(11) Kaiser, S. W. International Patent WO 86/04577, Aug. 14, 1986.

(12) Romannikov, V. N.; Ione, K. G. *Kinet. Catal.* **1984**, *25*, 75−80.

(13) Taylor, C. E.; Noceti, R. P.; Schehl, R. R. Direct Conversion of Methane to Liquid Hydrocarbons Through Chlorocarbon Interdiates. In *Methane Conversion*; Bibby, D. M., Chang, C. D., Howe, R. F., Yurchak, S., Eds.; Stud. Surf. Sci. Catal. 36; Elsevier Science: Amsterdam, 1988; pp 483−489.

(14) Jens, K.-J.; Halvorsen, S.; Bauman Ofstad, E. Methane Conversion Via Methyl chloride: Condensation of Methyl chloride to Light Hydrocarbons. In *Methane Conversion*; Bibby, D. M., Chang, C. D., Howe, R. F., Yurchak, S., Eds.; Stud. Surf. Sci. Catal. 36; Elsevier Science: Amsterdam, 1988; pp 491−495.

(15) Anderson, J. R. *Appl. Catal.* **1989**, *47*, 177−196.

(16) Lersch, P.; Bandermann, F. *Katalyse* **1989**, *118*, 183−201.

(17) Lersch, P.; Bandermann, F. *Appl. Catal.* **1991**, *75*, 133−152.

(18) White, C. M.; Douglas, L. J.; Hackett, J. P.; Anderson, R. R. *Energy Fuels* **1992**, *6*, 76−82.

(19) Sun, Y.; Cambell, S. M.; Lunsford, J. H.; Lewis, G. E.; Palke, D.; Tau, L.-M. *J. Catal.* **1993**, *143*, 32−44.

(20) Chich, B. *Rev. Roum. Chim.* **1997**, *42*, 1165−1170.

(21) Taylor, C. E. Conversion of Substituted Methanes over ZSM-Catalysts. In *Proceedings of the 12th International Congress on Catalysis*; Corma, A., Melo, F. V., Mendioroz, S., Fierro, J. L. G., Eds.; Stud. Surf. Sci. Catal. 130D; Elsevier Science: Amsterdam, 2000; pp 3633−3638.

(22) Jaumain, S.; Su, B.-L. Direct Catalytic Conversion of Chloromethane to Higher Hydrocarbons over Various Protonic and Cationic Zeolite Catalysts as Studied by in-situ FTIR and Catalytic Testing. In *Proceedings of the 12th International Congress on Catalysis*; Corma, A., Melo, F. V., Mendioroz, S., Fierro, J. L. G., Eds.; Stud. Surf. Sci. Catal. 130B; Elsevier Science: Amsterdam, 2000; pp 1607−1612.

(23) Brophy, J. H.; Font Freide, J. J. H. M.; Tomkinson, J. D. International Patent WO 85/02608, June 20, 1985.

(24) Murray, D. K.; Chang, J.-W.; Haw, J. F. *J. Am. Chem. Soc.* **1993**, *115*, 4732−4741.

(25) (a) Dahl, I. M.; Kolboe, S. *Catal.* Lett. **1993**, *20*, 329−336. (b) Dahl, I. M.; Kolboe, S. *J. Catal.* **1994**, *149*, 458−464. (c) Dahl, I. M.; Kolboe, S. *J. Catal.* **1996**, *161*, 304−309.

(26) (a) Mikkelsen, Ø.; Rønning, P. O.; Kolboe, S. *Microporous Mesoporous Mater.* **2000**, *40*, 95−113. (b) Arstad, B.; Kolboe, S. *Catal. Lett.* **2001**, *71*, 209−212. (c) Arstad, B.; Kolboe, S. *J. Am. Chem. Soc.* **2001**, *123*, 8137−8138. (d) Bjørgen. M.; Olsbye, U.; Kolboe, S. *J. Catal.*, in press.

(27) (a) Haw, J. F.; Nicholas, J. B.; Song, W.; Deng, F.; Wang, Z.; Xu, T.; Heneghan, C. S. *J. Am. Chem. Soc.* **2000**, *122*, 4763−4775. (b) Goguen, P. W.; Xu, T.; Barich, D. H.; Skloss, T. W.; Song, W.; Wang, Z.; Nicholas, J. B.; Haw, J. F. *J. Am. Chem. Soc.* **1998**, *120*, 2650−2651. (c) Sassi, A.; Wildman, M. A.; Ahn, H. J.; Prasad, P.; Nicholas, J. B.; Haw, J. F. *J. Phys. Chem. B* **2002**, *106*, 2294−2303. (d) Song, W.; Haw, J. F.; Nicholas, J. B.; Heneghan, C. S. *J. Am. Chem. Soc.* **2000**, *122*, 10726−10727. (e) Song, W.; Fu, H.; Haw, J. F. *J. Phys. Chem. B* **2001**, *105*, 12839−12843.

(28) (a) Seiler, M.; Schenk, U.; Hunger, M. *Catal. Lett.* **1999**, *62*, 139−145. (b) Hunger, M.; Seiler, M.; Buchholz, A. *Catal. Lett.* **2001**, *74*, 61−68.

(29) Alkylation of propene by chloromethane has been investigated experimentally by Kaeding and Butter. See: Kaeding, W. W.; Butter, S. A. U.S. Patent 3,906,054, Sept. 16, 1975.

(30) Frash, M. V.; van Santen, R. A. *Top. Catal.* **1999**, *9*, 191−205.

(31) Rozanska, X.; Saintigny, X.; van Santen, R. A.; Hutschka, F. *J. Catal.* **2001**, *202*, 141−155.

(32) Vos, A. M.; Rozanska, X.; Schoonheydt, R. A.; van Santen, R. A.; Hutschka, F.; Hafner, J. *J. Am. Chem. Soc.* **2001**, *123*, 2799−2809.

(33) Rozanska, X.; van Santen, R. A.; Hutschka, F.; Hafner, J. *J. Am. Chem. Soc.* **2001**, *123*, 7655−7667.

(34) Vos, A. M.; Nulens, K. H. L.; De Proft, F.; Schoonheydt, R. A.; Geerlings, P. *J. Phys. Chem. B* **2002**, *106*, 2026−2034.

(35) Rozanska, X.; Saintigny, X.; van Santen, R. A.; Clémendot, S.; Hutschka, F. *J. Catal.* **2002**, *208*, 89−99.

(36) Arstad, B.; Kolboe, S.; Swang, O. *J. Phys. Chem. B* **2002**, *106*, 12722−12726.

(37) Svelle, S.; Arstad, B.; Kolboe, S.; Swang, O. *J. Phys. Chem. B*, submitted for publication.

(38) (a) Dessau, R. M.; LaPierre, R. B. *J. Catal.* **1982**, *78*, 136−141. (b) Kolboe, S. *Acta Chem. Scand.* **1986**, *A40*, 711−713. (c) Dessau, R. M. *J. Catal.* **1986**, *99*, 111−116. (d) Song, W.; Marcus, D. M.; Fu, H.; Ehresmann, J. O.; Haw, J. F. *J. Am. Chem. Soc.* **2002**, *124*, 3844−3845.

(39) Frisch, M. J.; Trucks, G. W.; Schlegel, H. B.; Scuseria, M. A.; Robb, M. A.; Cheeseman, J. R.; Zakrzewski, V. G.; Montgomery, J. A.; Stratmann, R. E.; Burant, J. C.; Dapprich, S.; Millam, J. M.; Daniels, A. D.; Kudin, K. N.; Strain, M. C.; Farkas, O.; Tomasi, J.; Barone, V.; Cossi, M.; Cammi, R.; Mennucci, B.; Pomelli, C.; Adamo, C.; Clifford, S.; Ochterski, J.; Petersson, G. A.; Ayala, P. Y.; Cui, Q.; Morokuma, K.; Malick, D. K.; Rabuck, D. K.; Raghavachari, K.; Foresman, J. B.; Cioslowski, J.; Ortiz, J. V.; Stefanov, B. B.; Liu, G.; Liashenko, A.; Piskorz, P.; Komaromi, I.; Gomperts, R.; Martin, R. L.; Fox, D. J.; Keith, T.; Al-Laham, M. A.; Peng, C. Y.; Nanayakkara, A.; Gonzales, C.; Challacombe, M.; Gill, P. M. W.; Johnson, B. G.; Chen, W.; Wong, M. W.; Andres, J. L.; Head-Gordon, M.; Replogle, E. S.; Pople, J. A. *Gaussian 98 (revision A.11.)*; Gaussian, Inc.: Pittsburgh, PA, 1998.

(40) Hay, P. J.; Wadt, W. R. *J. Chem. Phys.* **1985**, *82*, 284−298.

(41) Check, C. E.; Faust, T. O.; Bailey, J. M.; Wright, B. J.; Gilbert, T. M.; Sunderlin, L. S. *J. Phys. Chem. A* **2001**, *105*, 8111−8116.

(42) Glukhovtsev, M. N.; Pross, A.; McGrath, M. P.; Radom, L. *J. Chem. Phys.* **1995**, *103*, 1878−1885.

(43) Basis sets were obtained from the Extensible Computational Chemistry Environment Basis Set Database, Version 10/29/02, as developed and distributed by the Molecular Science Computing Facility, Environmental and Molecular Sciences Laboratory, which is part of the Pacific Northwest Laboratory, P.O. Box 999, Richland, WA 99352, USA, and funded by the U.S. Department of Energy. The Pacific Northwest Laboratory is a multiprogram laboratory operated by Battelle Memorial Institute for the U.S. Department of Energy under Contract DE-AC06-76RLO 1830. Contact David Feller or Karen Schuchardt for further information. http://www.emsl.pnl.gov:2080/forms/basisform.html (accessed Oct. 2002).

(44) Thermodynamic data were taken from the NIST database; http://webbook.nist.gov/chemistry (accessed July 2002).

(45) Su, B.-L.; Jaumain, D. Chloromethane as a Probe Molecule to Characterize the Brönsted Acidity of Zeolites: An in-situ FTIR Study. In *Proceedings of the 12th International Zeolite Conference*; Treacy, M. M. J., Marcus, B. K., Bisher, M. E., Higgins, J. B., Eds.; Materials Research Society: Warrendale, PA, 1998; Vol. 4, pp 2689−2696.

(46) Sauer, J.; Ugliengo, P.; Garrone, E.; Saunders, V. R. *Chem. Rev.* **1994**, *94*, 2095−2160.

(47) Hammond, G. S. *J. Am. Chem. Soc.* **1955**, *77*, 334−338.

(48) The experimental proton affinities of chloride, bromide, and iodide are 1395, 1353, and 1315 kJ/mol.[44] Calculations at the B3LYP_ECP/6-31G(d) + ZPE level of theory yield 1356, 1322, and 1294 kJ/mol.

(49) Xia, X.-R.; Bi, Y.-L.; Wu, T.-H.; Zhen, K.-J. *Catal. Lett.* **1995**, *33*, 75−90.

(50) Kónya, Z.; Hannus, I.; Kiricsi, I. *Appl. Catal. B* **1996**, *8*, 391−404.

(51) Su, B.-L.; Jaumain, D.; Ngalula, K.; Briend, M. Effect of Acido-Basicity of Beta Zeolites on the Conversion of Chloromethane to Hydrocarbons as Studied by FTIR and TPD-MS. In *Proceedings of the 12th International Zeolite Conference*; Treacy, M. M. J., Marcus, B. K., Bisher, M. E., Higgins, J. B., Eds.; Materials Research Society: Warrendale, PA, 1998; Vol. 4, pp 2681−2688.

(52) Bosáček, V. *J. Phys. Chem.* **1993**, *97*, 10732−10737.

(53) Levik, O. I. Thesis, Norwegian Institute of Technology (now Norwegian University of Science and Technology), 1990.

(54) Olsbye, U.; Dahl, I. M. To be submitted for publication.